5366 *Chem. Mater.* **2010,** *22,* 5366–5370
DOI:10.1021/cm1017536

CHEMISTRY OF MATERIALS
Article

Evidence of Proton Transport in Atomic Layer Deposited Yttria-Stabilized Zirconia Films

Joong Sun Park,[†] Young Beom Kim,[†] Joon Hyung Shim,*[,†,§] Sangkyun Kang,[⊥] Turgut M. Gür,[‡] and Fritz B. Prinz[†,‡]

[†]*Department of Mechanical Engineering, and* [‡]*Department of Materials Science and Engineering, Stanford University, Stanford, California 94305,* [§]*Department of Mechanical Engineering, Korea University, Seoul, Korea, and* [⊥]*Samsung Advanced Institute of Technology, Samsung Electronics, Giheung, Gyeonggi-do, Korea*

Received June 23, 2010. Revised Manuscript Received August 10, 2010

This study presents spectroscopic and electrochemical evidence that verifies proton transport in the temperature regime 300−450 °C in yttria-stabilized zirconia (YSZ) thin film membranes fabricated by atomic layer deposition (ALD). High-resolution X-ray photoelectron spectrometry (XPS) of O1s showed that the OH peak was significantly more pronounced in ALD samples than in single-crystal YSZ. Similarly, secondary ion mass spectrometry (SIMS) measurements, conducted for comparison on single-crystalline YSZ and atomic layer deposited YSZ, indicated that ALD YSZ contains 100 times higher deuterium concentration than single crystalline YSZ. SIMS depth profiles suggested diffusion of protons through protonic defects in YSZ. We have also fabricated fuel cells employing ALD YSZ with dense palladium layers to block oxygen but allow hydrogen transport. These performed as protonic fuel cells at intermediate temperatures achieving 10 mW/cm^2 at 450 °C. These results open the possibility to engineer ALD YSZ as electrolyte membranes for new protonic devices operating at relatively low temperature regimes.

Introduction

Proton incorporation or transport in YSZ has initially been suggested by Wagner in the 1960s, who reported hydrogen diffusivity in YSZ single crystals at high temperatures and proposed the use of YSZ for high-temperature hydrogen sensing.[1,2] Also Guo et al.[3] observed high proton mobility through ZrO_2 grain boundaries at temperatures below 450 °C and attributed this to phase change from tetragonal to monoclinic zirconia. By contrast, however, there was only slight increase in the conductivity when cubic zirconia was exposed to wet environments.[4]

More recent reports have indicated that the nature and magnitude of conductivity in ceramics may greatly be affected by nanostructuring. Sata et al. reported enhanced ionic conductivity in alternating layers of CaF_2/BaF_2 heterostructures as the thickness of the layers approached tens of nanometers, which was attributed to increased charge carrier concentration by overlapping of space charge layers.[5] Similarly, Kosacki et al. found that conductivity noticeably increased in highly textured epitaxially grown films of yttria stabilized zirconia (YSZ) on MgO(100).[6] Interestingly, recent studies reported proton transport in nanocrystalline YSZ at temperatures below 150 °C when exposed to moisture.[7,8]

Normally, YSZ is an oxide ion conductor where oxide ions diffuse through the crystalline lattice via oxygen vacancies that are created for charge compensation upon doping by trivalent yttrium ions (Y^{3+}), which substitute for the quadrivalent zirconium ions (Zr^{4+}) in the cation sublattice.

In this context, observation of protonic conductivity in nanostructured YSZ is intriguing. Munir and co-workers have found that in wet air, YSZ nanopowders synthesized by coprecipitation method with average grain sizes ranging from 10 nm to 100 nm exhibited protonic conduction at low temperatures and the conductivity increased with decreasing grain size.[8−10] However, Guo et al. were not able to demonstrate proton conduction in nanostructured YSZ films that were fabricated by pulsed laser deposition (PLD) and annealed in water vapor at temperatures above 500 °C.[11]

The present study aims to help understand the inconsistency in the results of previous studies and verify the

*Corresponding author. E-mail: shimm@korea.ac.kr.

(1) Wagner, C. *Ber. Bunsenges Phys. Chem.* **1968**, *79*, 778.
(2) Stotz, S.; Wagner, C. *Ber. Bunsenges Phys. Chem.* **1967**, *79*, 781.
(3) Guo, X. *J. Phys. Chem. Solids* **1999**, *60*, 539.
(4) Guo, X. *Chem. Mater.* **2004**, *16*, 3988.
(5) Sata, N.; Eberman, K.; Eberl, K; Maier, J. *Nature* **2000**, *408*, 946.
(6) Kosacki, I.; Rouleau, C. M.; Becher, P. F.; Bentley, J.; Lowndesb, D. H. *Electrochem. Solid-State Lett.* **2004**, *7*(12), A459.
(7) Kim, S.; Anselmi-Tamburini, U.; Park, H. J.; Martin, M.; Munir, Z. A. *Adv. Mater.* **2008**, *20*, 556.
(8) Kim, S.; Avila-Paredes, H. J.; Wang, S.; Chen, C. T.; De Souza, R. A.; Martin, M.; Munir, Z. A. *Phys. Chem. Chem. Phys.* **2009**, *11*, 3035.
(9) Avila-Paredes, H. J.; Zhao, J.; Wang, S.; Pietrowski, M.; De Souza, R. A.; Reinholdt, A.; Munir, Z. Z.; Martin, M.; Kim, S. *J. Mater. Chem.* **2010**, *20*, 990.
(10) Anselmi-Tamburini, U.; Maglia, F.; Chiodelli, G.; Riello, P.; Bucella, S.; Munir, Z. A. *Appl. Phys. Lett.* **2006**, *89*, 163116.
(11) Guo, X.; Vasco, E.; Mi, S.; Szot, K.; Wachsman, E.; Waser, R. *Acta Mater.* **2005**, *53*, 5161.

Published on Web 08/25/2010

possibility of proton transport in nanograin size YSZ thin films fabricated by atomic layer deposition (ALD). It also aims to demonstrate that nanostructured or engineered architectures as well as the manner the material is synthesized or fabricated all affect transport properties as expected.[12]

For this purpose, we have fabricated nanograin thin YSZ films by ALD and characterized them with secondary ion mass spectrometry (SIMS) and X-ray photoelectron spectroscopy (XPS) in order to investigate proton transport in this material. In addition, electrochemical measurements were conducted using a solid oxide fuel cell (SOFC) arrangement with a nonporous oxide ion blocking layer placed between the catalyst and the YSZ electrolyte to demonstrate proton incorporation and transport in nanograin YSZ.

Experimental Section

Sample Preparation. YSZ films were fabricated using atomic layer deposition (ALD) by sequential deposition of its component oxides using metalorganic precursors. For this purpose, tetrakis(dimethylamido)zirconium(IV) (99.99% purity, Sigma-Aldrich), and tris(methylcyclopentadienyl)yttrium(III) (99.9% purity, Strem Chemicals) were used as precursors for ZrO_2, and Y_2O_3 deposition, respectively. Distilled water was used as the oxidant for each deposition cycle. Substrate temperature was set to 250 °C. The zirconium and yttrium precursors were heated to 75 and 190 °C, respectively. Deposition takes place in a customized ALD reactor described elsewhere.[13] Fabricated films were characterized via XPS (PHI VersaProbe 5000, Physical Electronics, USA), X-ray diffraction (XRD) (PANalytical X'Pert PRO, Philips, USA) and atomic force microscopy (AFM) (JSPM 5200, JEOL, Japan).

Isotope Experiment. To understand and verify proton incorporation into ALD YSZ, we performed hydrogen isotope exchange measurements in a deuterium oxide (D_2O) gas environment and the concentration of D in YSZ was measured by secondary ion mass spectrometry (ims7f SIMS, Cameca, France). For isotope exchange experiments, 70−80 nm thick ALD YSZ films were employed. These experiments involved evacuation of the vessel to at least 1×10^{-6} Torr pressure followed by the introduction of research grade (>99.9%) D_2O gas at 15Torr. The nanocrystalline YSZ films of grain sizes 20−30 nm as well as single-crystalline YSZ wafers were annealed at 20 °C - 450 °C for 3 h.

X-ray Photoelectron Spectroscopy. To investigate the chemical bonding state of oxygen in ALD YSZ, we performed high-resolution XPS to distinguish the metal−oxygen bond from hydroxyl bonding in the films. XPS scanning was performed between 520 eV and 540 eV with 0.1 eV energy step.

Fuel Cell Fabrication. Si-based MEMS processing methods were used for the fabrication of the fuel cell structure. 150−200 nm thick ALD YSZ films were deposited on Si_3N_4 patterned wafers followed by chemical etching of the silicon substrate in KOH solution leaving behind a freestanding structure. Supporting Si_3N_4 layer was removed by plasma etching. A 300 nm thick dense palladium layer, which allows rapid diffusion of protons but blocks oxide ion transport was deposited by electron beam evaporation on both sides of the ALD YSZ membrane layer. Subsequently, 80 nm thick platinum layer was deposited by DC sputtering to serve as catalyst and current collector. .

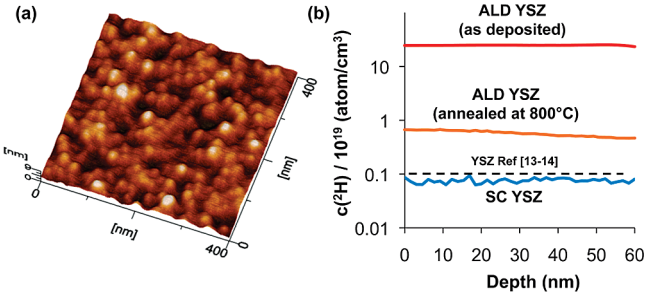

Figure 1. (a) AFM topography of ALD YSZ (average grain size ~20 nm), (b) SIMS depth profiles of deuterium in as-deposited, and 800 °C annealed ALD YSZ films resulting in an average deuterium concentration of $\sim 2 \times 10^{20}$ cm^{-3}.

Results and Discussion

XPS characterization of the ALD YSZ films indicated that YSZ films contained 7−8 mol % yttria, which is about the optimal doping content for oxide ion conductivity.[14−16] AFM topography measurements indicated that ALD YSZ films have nanogranular structure with grain size around 20 nm as depicted Figure 1a. Similarly, XRD and TEM analyses of ALD YSZ films reported earlier[13] showed as-deposited films have nanocrystalline cubic structure in an amorphous matrix, and film crystallinity increased with increasing postannealing temperature to yield a completely polycrystalline microstructure at 800 °C.

To investigate proton incorporation, ALD YSZ films were annealed in D_2O environment followed by SIMS analysis. The depth profile shown in Figure 1b clearly indicates the presence of deuterium in the ALD YSZ films annealed at 300 °C during D_2O exchange experiments. Likely due to fast diffusion of deuterium in the ALD films, the concentration of deuterium estimated to be $\sim 2 \times 10^{20}$ atom.cm^{-3} inside the films was nearly constant over the depth probed by SIMS. In addition, this value of 2.5×10^{20} atom.cm^{-3} is nearly 2 orders of magnitude higher than that previously reported ($\sim 1 \times 10^{18}$ atom cm^{-3}) by Wagner.[1,2] Similarly, SIMS analysis of the single-crystalline YSZ sample, which does not contain grain boundaries, indicated over 100 times smaller concentration of deuterium. We speculate that this enhancement may in part be attributed to high grain boundary density in ALD YSZ films.

Indeed, recent studies demonstrated nearly 3 orders of magnitude faster diffusion of oxygen along grain boundaries in nanogranular (< 100 nm) 6.9 mol % YSZ samples than for single crystal 9.5 mol % YSZ.[17,18] In good

(12) Gür, T. M. *Adv. Mater.* **1996**, *8*(11), 883.
(13) Shim, J.; Chao, C.; Huang, H.; Prinz, F. *Chem. Mater.* **2007**, *19*, 3850.
(14) Kuwabara, M.; Murakami, T.; Ashizuka, M.; Kubota, Y.; Tsukidate, T. *J. Mater. Sci. Lett.* **1985**, *4*, 467.
(15) Pornprasertsuk, R.; Panchapakesan, R.; Charles, B. M.; Fritz, B. P. *J. Appl. Phys.* **2005**, *98*, 103513.
(16) Steele, B. C. H. *Solid State Ionics* **1995**, *75*, 157.
(17) Knoner, G.; Reimann, K.; Rower, R.; Sodervall, U.; Schaefer, H. E. *Proc. Natl. Acad. Sci. U. S. A.* **2003**, *100*, 3870.
(18) Brosmann, U.; Kröner, G.; Schaefer, H.-E.; Würschum, R. *Rev. Adv. Mater.* **2004**, *6*, 7.

agreement with the results of the present work, the observed enhancement was attributed to the formation of vacancy-type free volume within the grain boundaries that facilitate faster diffusion along grain boundaries in YSZ.[19] These results collectively suggest that high grain boundary densities, i.e., small grain size in the nanoscale regime, seem to promote faster proton transport pathways.

We have also observed that the concentration of deuterium decreased significantly when the ALD YSZ films were annealed at 800 °C in air for 2 h (see Figure 1b). The differences between the two ALD YSZ samples that originally contained protons were in effect the degree of crystallinity and temperature history, where the former clearly depends on the latter. As evidenced by XRD analysis, the film started to show crystallization after annealing at high temperature. On the basis of the SIMS and XRD results, we propose that temperature history and the degree of film crystallinity may be important considerations for proton transport. This is in general agreement with the shift commonly observed in the transference numbers for protons and oxide ions as well as their ionic conductivities in doped cerates (e.g., Gd-doped $BaCeO_3$) from primarily a proton-conducting regime at low temperatures to a predominantly oxide ion-conducting regime at high temperatures because of gradual loss of protons from the lattice.[20,21] Although the effect of temperature can be rationalized and explained by loss of protons (or dehydration), the details of the mechanism behind the effects of crystallinity and grain boundary density on proton transport is not well understood or established. Also, it is difficult to decouple the effects of temperature and crystallinity, which are interdependent.

We speculate that the mechanism of proton incorporation into YSZ, which has a cubic fluorite structure, is likely to be similar to that for doped perovskites of the general formula ABO_3. Accordingly, water incorporation into YSZ may proceed via reaction 1 expressed in Kröger–Vink notation

$$H_2O + V_O^{\bullet\bullet} + O_O^X \rightarrow 2(OH)_O^{\bullet} \quad (1)$$

where, $V_O^{\bullet\bullet}$ denotes an oxygen vacancy in the oxygen sublattice in YSZ with a relative charge of +2, O_O^X represents neutral oxygen in its normal lattice site in YSZ, and $(OH)_O^{\bullet}$ is the protonic defect associated with a lattice oxygen in YSZ with an effective charge of +1. In the case of doped perovskites such as Y- or Gd-doped $BaCeO_3$, proton transport in the bulk occurs via a two-step Grotthuss mechanism involving first a rotational diffusion of the proton defect around the oxide ion in the lattice followed by hopping to a neighboring oxide ion site.[22,23] We assume that this mechanism may also be valid for bulk, or intragrain, transport of protons in YSZ.

Guo[4] has recently reviewed the various degradation mechanisms proposed in the literature for tetragonal ZrO_2 when it is exposed to water vapor (or moisture) at relatively low temperatures. On the basis of these results, the proton transport mechanism proposed by Guo[3,4] for tetragonal zirconia includes the following steps: (i) chemical absorption of water on ZrO_2 surface; (ii) reaction of water with surface O^{2-} to form hydroxyl, OH^-, groups; (iii) diffusion of OH^- through grain boundaries; and (iv) filling of oxygen vacancies by OH^- ions to form protonic defects. Because ALD-fabricated YSZ films have grain sizes in the 20−30 nm range, the resulting high density of grain boundaries provide effective pathways for OH^- for incorporation and transport as also suggested by Kim et al.[8] It is also reported that oxygen vacancy concentration in the space charge regions near the grain boundaries in YSZ increases with decreasing grain size,[24] providing further support for the behavior observed in nanograin YSZ films fabricated by ALD in the present study.

In addition, we note that the method of synthesis is another important consideration that is expected to affect transport properties.[12] We speculate that the observed proton transport in YSZ films may be attributed to the innate characteristics of ALD, which is a low-temperature deposition process, and also where water vapor is employed as the oxidant for the metalorganic precursors during the fabrication of the YSZ films. The YSZ nanograins at the low fabrication temperature of ALD likely provide favorable sites near the grain boundaries for water absorption and proton transport, possibly through the OH^- groups. By contrast, PLD requires elevated temperatures that result in loss of surface OH^- groups, and this can account for why significant proton transport was not observed in YSZ films prepared by PLD, although these films also had nanocrystalline YSZ grains.[10] So it seems that synthesis conditions play a role for the observed proton transport in ALD YSZ films.

In addition to SIMS analysis, high-resolution XPS measurements were performed in order to provide independent evidence for the presence of protons in the nanograin YSZ films. Figure 2 showed high-resolution XPS results of O1s in the nanograin ALD YSZ film and the commercially available single crystalline (SC) YSZ after annealing in wet environment (15Torr of H_2O) at 300 °C. The XPS spectra consist of two distinct loops. The one at the lower binding energy is characteristic of oxygen ion (O^{2-}) in the oxide, and the other loop corresponds to hydroxyl ions (OH^-). Accordingly, we suggest that proton transport in ALD YSZ likely occurs, via the Grotthuss mechanism described above, through protonic defects created by oxygen vacancies as represented in reaction 1. Because the XPS spectra were obtained after a few minutes of argon etching corresponding to tens of nanometer in depth, sampling from this depth in the film provides clear evidence of the presence of protons in the YSZ grains. For all practical purposes, the chance that the observed OH^- peak in the spectra may come from

(19) Würschum, R.; Shapiro, E.; Dittmar, R.; Schaefer, H. E. *Phys. Rev. B: Condens. Matter* **2000**, *62*, 12021.
(20) Taniguchi, N.; Hatoh, K.; Niikura, J.; Gamo, T.; Iwahara, H. *Solid State Ionics* **1992**, *998*, 53.
(21) Bonanos, N. *Solid State Ionics* **1992**, *967*, 53.
(22) Kreuer, K. D. *Annu. Rev. Mater. Res.* **2003**, *33*, 333.
(23) Merinov, B.; Goddard, W., III. *J. Chem. Phys.* **2009**, *130*, 194707.
(24) Guo, X.; Zhang, Z. *Acta. Mater.* **2003**, *51*, 2539.

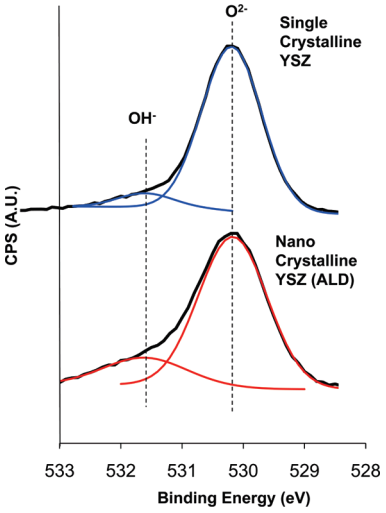

Figure 2. High-resolution XPS spectra of O1s in single-crystalline YSZ and ALD (nanocrystalline) YSZ. The higher-energy band corresponds to OH^- and the lowe-energy band corresponds to O^{2-}.

moisture in the high vacuum analytical chamber of the XPS instrument, or carried from prior exposure to air can be dismissed. For nonannealed samples, only low binding energy peaks were observed suggesting that the presence of OH^- ions mainly resulted from the wet annealing process. The area ratio of the OH^- peak to the O^{2-} peak indicates the relative amounts of OH^- in the films. It was found that the area ratio was three times higher for ALD YSZ films than in the single crystalline YSZ. The area ratio (~0.21) in ALD YSZ films is comparable to that of tetragonal zirconia, which degrades at low temperatures because of volume expansion during phase transformation and is known to have higher proton solubility than cubic YSZ.[4]

For electrochemical verification of protonic transport, thin film solid oxide fuel cell structures based on ALD YSZ electrolyte membrane were fabricated using silicon micromachining processing. To block oxygen and restrict its involvement during fuel cell operation, a gastight dense oxygen barrier layer made of a mixed electronic protonic conducting metal was inserted between the platinum catalyst and the YSZ electrolyte. Palladium, which allows proton transport but blocks oxygen, was chosen as the barrier interlayer. Hydrogen is known to transport rapidly through palladium by lattice strain gradient induced diffusion, i.e., Gorsky effect,[25,26] and its diffusion rate is sufficiently high that it is not expected to be rate limiting during electrochemical measurements. The scanning electron microscope cross-section image of this fuel cell structure is shown in Figure 3.

Cell performance of palladium-coated SOFC structures featuring ALD YSZ electrolyte membrane was tested in an experimental fixture previously described elsewhere.[27] Pure hydrogen was supplied to the anode, whereas the cathode was exposed to ambient air. Measured open circuit voltages (OCV) ranged from 600 mV up to 810 mV between 300 and 450 °C, slightly lower than theoretically expected. We speculate that the reason for the low OCVs may be due to the formation of palladium oxide at the cathode, which results in a decrease in OCV values. Indeed, established thermochemical data[28] clearly indicate that palladium oxide is expected to form at the air side of the fuel cell at the cell operating temperatures and oxygen partial pressure. This was also confirmed by XPS analysis. The relevant stability regimes in van't Hoff representation and detail spectroscopic results are provided in the Supporting Material section. Nevertheless, the ALD YSZ cell displayed typical fuel cell behavior as shown in Figure 4. Maximum power densities increased from 0.5 to 10 mW/cm^2 as the temperature was raised from 300 to 450 °C. By contrast, the fuel cell featuring YSZ fabricated by the PLD method did not even exhibit an open circuit voltage or electrical current using the same experimental setup and testing procedure. These results demonstrate that method of fabrication clearly affect transport properties.

To the best of our knowledge, this is the first successful demonstration of an intermediate temperature solid oxide fuel cell based on YSZ electrolyte that was operated

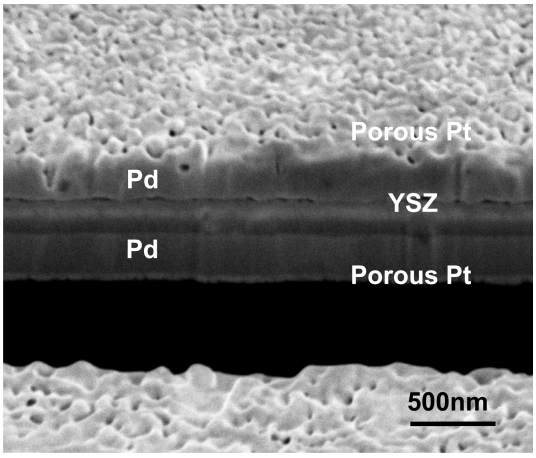

Figure 3. Scanning electron microscope (SEM) image of the ALD YSZ fuel cell element.

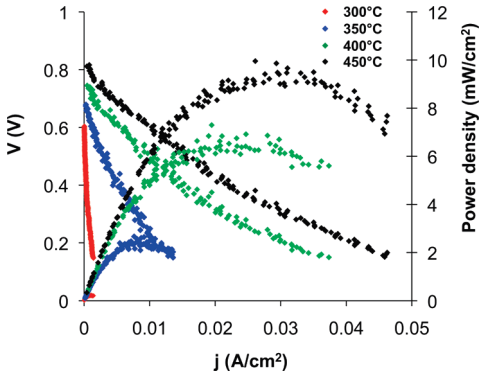

Figure 4. Current−voltage characteristic of the protonic ALD YSZ-based hydrogen/air fuel cell operating at 300−450 °C.

(25) Lewis, F. A.; Magennis, J. P.; McKee, S. G.; Ssebuwufu, P. J. M. *Nature* **1983**, *306*, 673.
(26) Lewis, F. A.; Baranowski, B.; Kandasamy, K. *J. Less-Common Met.* **1987**, *134*, L27.
(27) Huang, H.; Nakamura, M.; Su, P.; Fasching, R.; Saito, Y; Prinz, F. B. *J. Electrochem. Soc.* **2007**, *154*, B20.
(28) Barin, I. *Thermochemical Data of Pure Substances*, 3rd ed.; VCH: Weinheim, Germany, 1995.

in a proton transport mode. Lack of other examples from the literature make it difficult to compare the fuel cell performance results reported here with other ceramic fuel cells based on fluorite structure electrolytes. However, we can place this performance level of 10mW/cm^2 at 450 °C in the context of protonic fuel cells that employ anhydrous perovskite-based doped ceramics. In this regard, Peng et al. recently reported less than 4 mW/cm^2 at 800 °C with a protonic fuel cell employing 1 mm thick BYZ with porous Pt electrodes, and 25 mW/cm^2 with 10 μm thick ZnO-doped BYZ membrane at the same elevated temperature.[29] In a similar study using protonic fuel cells, Traversa and co-workers obtained power densities of 7mW/cm^2 at 700 °C with 0.6 mm thick BYZ,[30] and more recently, 110 mW/cm^2 at 600 °C from a cell employing pulsed laser deposited BYZ membrane.[31] A more recent study demonstrated 170 mW/cm^2 at 700 °C using a 20 μm thick BYZ membrane on NiO/$BaZr_{0.1}Ce_{0.7}Y_{0.2}O_3$ cermet anode support with a $Sm_{0.5}Sr_{0.5}CoO_3$−$Ce_{0.8}Sm_{0.2}O_2$ composite cathode.[32]

These comparative results demonstrate that the performance of our YSZ-based protonic fuel cells in the relatively low temperature regime of 300−450 °C compares favorably with many of proton conducting ceramic fuel cell results based on yttria doped barium zirconate measured at much higher temperatures. This makes nanograin ALD YSZ structures attractive for potential protonic devices. Furthermore, its excellent stability against CO_2 attack provides YSZ-based protonic fuel cells added advantage over protonic fuel cells based on doped barium zirconate and barium cerate membranes, which are known to exhibit susceptibility toward carbonate formation upon reaction with ambient CO_2.[22]

(29) Peng, C.; Melnik, J.; Li, J.; Luo, J.; Sanger, A. R.; Chuang, K. T. *J. Power Sources* **2009**, *190*, 447.
(30) D'Epifanio, A.; Fabbri, E.; Di Bartolomeo, E.; Licoccia, S.; Traversa, E. *Fuel Xells* **2008**, *8*, 69.
(31) Pergolesi, D.; Fabbri, E.; Traversa, E. Abstract submitted to the 218th Meeting of The Electrochemical Society, Las Vegas Oct 10−15, **2010**.
(32) Sun, W.; Yan, L.; Shi, Z.; Zhu, Z.; Liu, W. *J. Power Sources* **2010**, *195*, 4727.

Summary

We have successfully demonstrated and provided experimental and analytical evidence for proton incorporation and protonic transport in nanograin YSZ films fabricated by ALD technique. SIMS measurements coupled to isotope exchange experiments verified proton incorporation and diffusion into the ALD YSZ films that are otherwise well-known conductors of oxide ions. Also high-resolution XPS results indicated a significantly higher population of OH^- in ALD YSZ films than in single-crystal YSZ, suggesting preponderance of proton diffusion via protonic defects along the grain boundaries. More importantly, solid oxide fuel cells employing ALD YSZ membranes with dense palladium barrier interlayers for blocking oxide ions have been operated successfully as protonic ceramic fuel cells, and achieved power densities up to 10 mW/cm^2 at 450 °C for the first time.

Acknowledgment. We are grateful to Dr. Yunbin Guan and Prof. John Eiler of the Geology department at California Institute of Technology for their assistance and collaboration on the SIMS work. This material is based on works partially supported by a Samsung Scholarship (J.S.P.).

Note Added after ASAP Publication. The Supporting Information was missing in the version published ASAP August 25, 2010; the corrected version was published ASAP August 27, 2010.

Supporting Information Available: Additional information (PDF). This material is available free of charge via the Internet at http://pubs.acs.org.